# Exciton localization and quantum efficiency—A comparative cathodoluminescence study of (In,Ga)N/GaN and GaN/(Al,Ga)N quantum wells

U. Jahn,[a] S. Dhar, O. Brandt, H. T. Grahn, and K. H. Ploog
*Paul-Drude-Institut für Festkörperelektronik, Hausvogteiplatz 5–7, 10117 Berlin, Germany*

I. M. Watson
*Institute of Photonics, University of Strathclyde, Wolfson Centre, 106 Rottenrow, Glasgow G4 0NW, United Kingdom*

(Received 9 September 2002; accepted 23 October 23 2002)

We study the quantum efficiency ($\eta$) and transition energy ($E_t$) as a function of excitation density and temperature in (In,Ga)N/GaN multiple quantum wells (MQWs) fabricated by molecular-beam epitaxy (MBE) and metal-organic chemical-vapor deposition (MOCVD), as well as in an MBE-grown GaN/(Al,Ga)N MQW. A method based on cathodoluminescence spectroscopy is proposed to be suitable for a reproducible measurement of the power dependence of $\eta$ and $E_t$. The experimental results are fit to a recently developed model allowing for a distinction of localization and electric-field effects for $\eta$ and $E_t$, as well as for the extraction of the localization energy, density of localization centers, and radiative recombination rate of localized excitons. In the (In,Ga)N/GaN MQWs grown by MBE and MOCVD, we found a value of the localization energy of 34 and 100 meV, respectively. In the MBE-grown GaN/(Al,Ga)N MQW, the exciton recombination is dominated by quasifree excitons even at low temperatures. © *2003 American Institute of Physics.* [DOI: 10.1063/1.1529993]

## I. INTRODUCTION

It is generally accepted that the quantum efficiency $\eta$ and the optical transition energy $E_t$ of GaN-based heterostructures such as (In,Ga)N/GaN and GaN/(Al,Ga)N quantum wells (QWs) are reduced by piezoelectric and spontaneous polarization fields via the quantum-confined Stark effect (QCSE).[1,2] Thus, electric-field screening by free carriers originating from doping, optical generation, or electric injection can result in significant modifications of the optical properties of otherwise identical QW structures. A complete screening of the electric field is expected to be achieved only for very high-carrier densities.[3,4] Furthermore, exciton localization within minima of the lateral QW potential leads also to a decrease of $E_t$, but to an increase of the quantum efficiency. Localization effects are believed to play an essential role in (In,Ga)N/GaN QWs, where large energy variations are caused by lateral fluctuations of the InN mole fraction.[5,6] Since the fraction of localized excitons of a given QW structure varies with temperature and carrier density, the impact of localization effects on the optical properties depends on the excitation and doping conditions.[7,8]

Electric fields and localization act also as a combined effect on $\eta$ and $E_t$, since the depths of the potential minima are enhanced by electric fields due to higher strain within regions of larger InN mole fraction.[9] The influence of either effect—QCSE or localization—on the optical properties depends on the well width,[10] growth method and conditions, temperature, as well as on the excitation conditions. In any case, both effects act simultaneously[1,9,11] and can hardly be disentangled by experiments. In many studies, the decay time of the luminescence intensity as a function of temperature and energy is used to obtain access to the actual origin of the complex recombination dynamics in (In,Ga)N/GaN[10,12–17] and GaN/(Al,Ga)N QWs.[3,18–20] Another approach is to investigate $E_t$ as a function of the well width and to compare the respective data with results of a self-consistent solution of the Schrödinger and Poisson equations as has been done in several studies for the (In,Ga)N/GaN[11,17,21] and GaN/(Al,Ga)N system.[2,3,22–25]

The dependence of the quantum efficiency on excitation density has rarely been investigated despite its potential to provide a comprehensive picture about the contributions of carrier localization, electric-field screening, and nonradiative recombination channels.[26] The difficulties of power-dependent measurements are at least twofold. First, there is a lack of accurate knowledge about the actual density of excited carriers in photoluminescence (PL) or electroluminescence experiments. Second, GaN-based heterostructures show electrical and optical metastabilities after high-power exposure, which can significantly distort the excitation density dependence of the PL intensity. Recently, several authors reported on a pronounced persistent photoconductivity[27–34] and on a so-called optical memory effect, where a change of the luminescence properties due to a high-power exposure with UV light or electrons is preserved for hours or even days.[35–37] Chang *et al.*[38] suggested that both effects have the same origin. Consequently, optical investigations associated with an exposure of the sample by UV light or electrons are expected to be affected by the measurement itself.

[a]Electronic mail: ujahn@pdi-berlin.de

 

TABLE I. Sample number, material system, growth method, well width ($d_W$), barrier width ($d_B$), and number of periods for the samples investigated.

| Sample | Material | Growth | $d_W$ (nm) | $d_B$ (nm) | Periods |
|---|---|---|---|---|---|
| 1 | $In_{0.16}Ga_{0.84}N/GaN$ | MBE | 3.1 | 12.1 | 10 |
| 2 | $In_{0.17}Ga_{0.83}N/GaN$ | MBE | 5.9 | 8.8 | 10 |
| 3 | $In_{0.10}Ga_{0.90}N/GaN$ | MOCVD | 2.6 | 7.0 | 10 |
| 4 | $GaN/Al_{0.15}Ga_{0.85}N$ | MBE | 2.3 | 8.0 | 15 |

In this paper, we propose a simple method to access the power dependence of the quantum efficiency of GaN-based QWs by cathodoluminescence (CL) investigations. The basic idea behind our approach is the variation of the density of excited carriers by changing the excitation volume, while the power of the electron beam is kept constant. Since in this way the total number of excited carriers is also constant during the experiment, the recorded CL intensity is a direct measure for $\eta$. Moreover, the proposed method allows for a reproducible measurement of the density dependence under well-defined conditions. In conjunction with a recently developed model describing the recombination dynamics of free and bound excitons and incorporating polarization-field screening in a realistic manner,[26] this method allows for the determination of the radiative recombination rate of free excitons, including their activation energy as well as the density of bound excitons. The power dependence of $\eta$ is complemented by temperature-dependent measurements. In order to investigate the different degrees of localization, we applied the method to (In,Ga)N/GaN multiple quantum wells (MQWs) grown by molecular-beam epitaxy (MBE) and metal-organic chemical-vapor deposition (MOCVD), which due to the different growth temperatures exhibit different degrees of the lateral variation of the InN mole fraction. In addition, a GaN/(Al,Ga)N MQW structure grown by MBE is studied to remove the influence of composition fluctuations in the well layer on exciton localization. We compare the results for these three systems in order to obtain a unified picture about the impact of exciton localization, electric-field screening, and non-radiative recombination on the quantum efficiency of these material systems, which exhibit very different physical properties.

## II. EXPERIMENTAL PROCEDURE

Three types of samples have been investigated: (In,Ga)N/GaN and GaN/(Al,Ga)N multiple quantum wells (MQWs) grown by plasma-assisted and reactive MBE on 6H–SiC substrates, respectively, as well as an (In,Ga)N/GaN MQW grown by MOCVD on sapphire. Details of the growth are given elsewhere.[3,10,39] The layer parameters are summarized in Table I. The thickness of the QWs cover a range between 2.3 and 5.9 nm.

Cathodoluminescence investigations were performed in a scanning electron microscope (SEM) equipped with an Oxford mono-CL2 and He-cooling stage operating at temperatures between $T=5$ and 300 K. A grating monochromator and a cooled charge-coupled device array were used to disperse and detect the CL signal, respectively. In order to get access to the quantum efficiency as a function of the excitation density, the excitation volume is varied by defocusing the electron beam in reproducible steps, while the total number of generated electron-hole pairs, i.e., the energy and the current of the electron beam, are kept constant. The scanned sample area is always set to $20\times20$ $\mu m^2$. The selected scan resolution and scan time of $512\times512$ points and 125 ms, respectively, result in a dwell time of the electron beam per spot of about 500 ns. In this way, the actual value of the generation rate $G$ of carriers per unit area depends only on the spot size of the electron beam, which in turn is determined by the degree of defocusing of the SEM. Figure 1 shows the spot area as a function of the degree of defocusing, where for each data point the focus button of the SEM has been changed by five steps. In the displayed range, the excitation area varies by more than two orders of magnitude. The respective spot area is measured by exposing a resist layer as used for electron-beam lithography. Five examples are shown in the inset of Fig. 1 ranging from the focused beam to a degree of defocusing, which corresponds to 65 steps. Within the sensitivity of the electron resist, the exposure dose is found to be homogeneously distributed even for a strongly defocused electron beam. The number of generated electron-hole pairs per second can be expressed as[40]

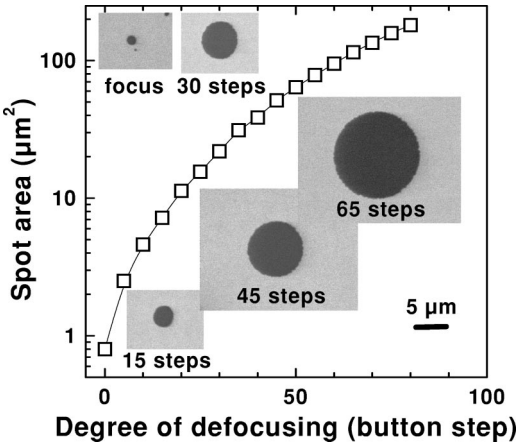


FIG. 1. Spot area of the electron beam as a function of the degree of defocusing. The area has been determined by exposing an electron resist for different steps of the focus button. The inset shows five examples ranging from the focused electron beam to a degree of defocusing, which corresponds to 65 button steps. The scale marker is valid for all images.

$$G_0 = 6.25\times10^{21} V_0 I_b \frac{1-\delta\times\overline{V}/V_0}{\epsilon}, \tag{1}$$

where $V_0$ is the beam energy in keV, $I_b$ the beam current in A, $\delta\simeq0.2$ the fraction of backscattered electrons, $\overline{V}\simeq0.65\ V_0$ the mean energy of the backscattered electrons in keV, and $\epsilon\simeq10$ eV the mean energy required to generate an electron-hole pair. For the estimation of $G$ (generation rate per unit area and second in a single QW), we assume that all the excited carriers are captured within the well layers before they recombine and $G=G_0/(AN)$, where $A$ denotes the spot area and $N$ the number of QWs situated within the depth of the scattering of the primary electron beam. The latter is

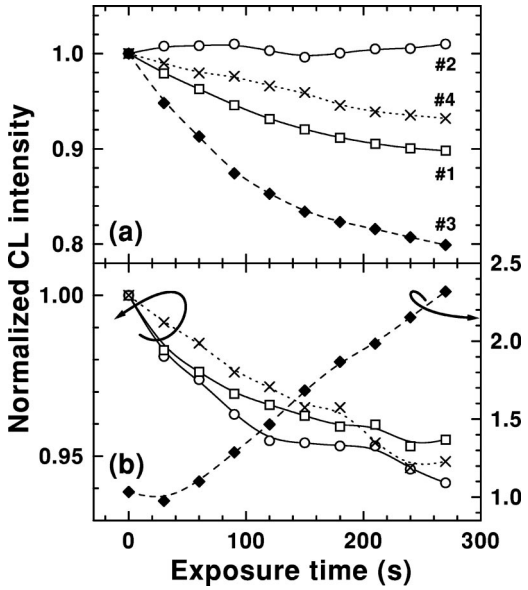


FIG. 2. Integrated CL intensity of samples 1 to 4 as a function of the electron-beam exposure time for (a) 5 K and (b) 300 K. The beam current and energy amounted to 0.25 nA and 5 keV, respectively.

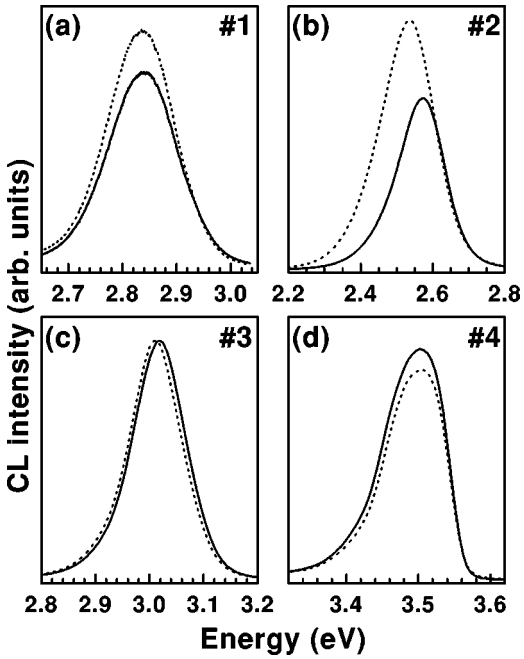


FIG. 3. CL spectra of samples (a) 1, (b) 2, (c) 3, and (d) 4 excited with the focused (solid lines) and strongly defocused (dotted lines) electron beam. In (a), the focused and defocused beam correspond to $G=6\times10^{19}$ and $4\times10^{17}$ $cm^{-2}\,s^{-1}$, respectively. In (b) to (d), the focused and defocused beam correspond to a value of $G$ of about $1\times10^{19}$ and $1\times10^{17}$ $cm^{-2}\,s^{-1}$, respectively.

determined by Monte Carlo simulations, using the commercial program MC-SET developed by E. Napchan (DLM Enterprise).

Two parameters have to be carefully examined to determine whether they remain constant, while defocusing the electron beam. These are the collection efficiency of the CL mirror and the electron-beam current. The latter remains constant within a much wider range of the degree of defocusing than used in our measurements. However, the CL collection efficiency is the limiting factor. It remarkably decreases, when the area of the scanned sample region increases, as a result of a strongly defocused electron beam. We have identified the range of constant collection efficiency and restricted the defocusing to this range. Since the total number of generated electron-hole pairs is not changed, when the generation rate is varied by means of the proposed method, the acquired CL intensity is a direct measure for the quantum efficiency $\eta$ as a function of excitation density. The $T$ dependence of $\eta$ was studied by CL and photoluminescence (PL) experiments. For the latter, we used a He–Cd-laser operating at a wavelength of 325 nm as the excitation source.

## III. RESULTS AND DISCUSSION

### A. Excitation density dependence of quantum efficiency

In order to estimate the actual influence of optical metastabilities on the measurements as mentioned above for all four samples, we acquired CL spectra for samples 1 to 4 as a function of electron-beam exposure time using the focused electron beam. The beam energy and current amounted to 5 keV and about 0.25 nA, respectively, which correspond to the values usually chosen for the experiments discussed below. In Figs. 2(a) and 2(b), the normalized intensity of the near-band-gap CL is plotted as a function of the exposure time for $T=5$ and 300 K, respectively. At low $T$, the CL intensity either remains constant (sample 2) or decreases gradually and eventually tends to saturate (samples 1, 3, and 4) with increasing electron exposure time. While the MBE-grown MQWs exhibit a maximum decrease of the CL intensity of about 10%, the CL intensity of the MOCVD-grown sample 3 is reduced by at least 20%. At 300 K, the MBE-grown samples show a negligible decrease of the CL intensity of about 5%. In the MOCVD-grown MQW, however, we observe a steep increase of the CL intensity by more than a factor of 2. The physical background of this phenomenon is not the subject of this article, but we have to take those effects into account for the interpretation of our experimental results.

Figures 3(a)–3(d) display the CL spectra of the samples obtained at 5 K for high (solid line) and low (dotted line) generation rates corresponding to a focused and strongly defocused electron beam, respectively. The comparison of the solid and dotted spectra indicates the variation of $\eta$, when the generation rate is varied by more than two orders of magnitude. Here, exposure effects can be neglected, since the two spectra have been acquired within a rather short exposure time. For the 3-nm- and 6-nm-thick (In,Ga)N/GaN QWs grown by MBE [samples 1 and 2 in Figs. 3(a) and 3(b), respectively], an increase of $G$ results in a decrease of the quantum efficiency and causes a blueshift of the spectra. In the MOCVD-grown (In,Ga)N/GaN MQW [sample 3 in Fig. 3(c)], $\eta$ and $E_t$ change only very little with $G$. However, in the GaN/(Al,Ga)N MQW [sample 4 in Fig. 3(d)], $\eta$ varies in the opposite direction as for the MBE-grown (In,Ga)N/GaN MQWs (samples 1 and 2), and no spectral shift is observed with an increasing generation rate. The dependence in Figs.

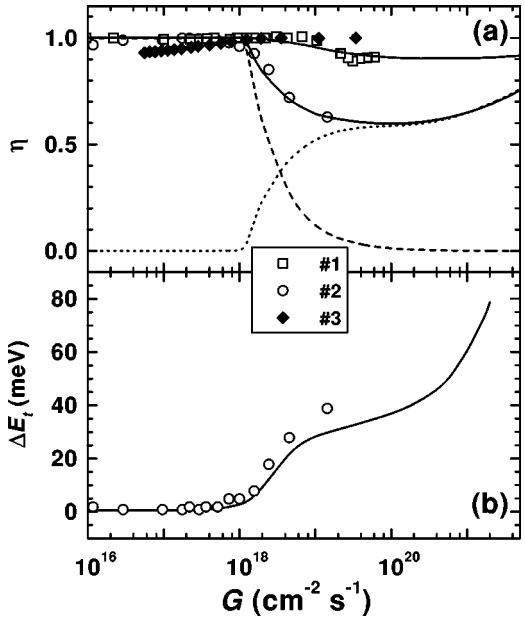


FIG. 4. (a) Quantum efficiency $\eta$ and (b) shift of the optical transition energy $\Delta E_t$ as a function of $G$ at 5 K. The lines indicate the fits to a recently developed model, where the solid lines correspond to the total quantum efficiency of samples 1 and 2 in (a) and to $\Delta E_t$ of sample 2 in (b). In (a), the dotted and dashed lines depict the quantum efficiency of the free and localized excitons, respectively.

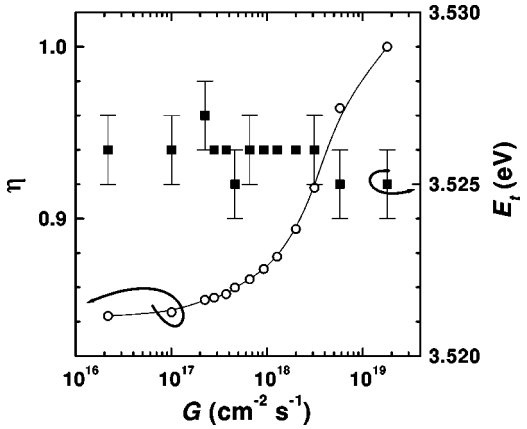


FIG. 5. Quantum efficiency and optical transition energy of sample 4 as a function of $G$ at 5 K.

3(a) and 3(b) can only be explained by a saturation of localized exciton states and not by screening of the piezoelectric field. The dependence of $\eta$ on $G$ observed in the GaN/(Al,Ga)N MQW is also not due to electric-field screening, since no spectral shift is observed with increasing generation rate.

Figure 4(a) displays the dependence of $\eta$ on the generation rate for samples 1 to 3 at 5 K. The measurements were performed with the focused electron beam (high generation rates) first and proceeded towards low values of $G$. Thus, the gradual increase of the quantum efficiency with decreasing $G$ cannot be a result of degradation by electron-beam exposure, which would lead to the opposite behavior. Moreover, the 6 nm MQW (sample 2) appears to be insensitive to the exposure of the electron beam, but shows the largest increase of $\eta$ with a decreasing generation rate. Consequently, Fig. 4(a) reflects the actual dependence of $\eta$ on excitation density and confirms the results shown in Figs. 3(a), 3(b), and 3(c). Assuming that for low excitation densities localized exciton states are exclusively occupied and nonradiative recombination channels are completely suppressed, we normalize $\eta$ at low values of $G$ to unity. As has been shown in Fig. 3(c), $\eta$ for sample 3 hardly varies within the measured range of the generation rate. The respective $G$ dependence of the quantum efficiency [diamonds in Fig. 4(a)] exhibits merely a small reduction of $\eta$ of about 7% for $G<10^{18}$ $\mathrm{cm}^{-2}\,\mathrm{s}^{-1}$. This reduction of $\eta$ is rather due to a degradation caused by the electron-beam exposure than to an actual excitation density effect (cf. Fig. 2). Compared with the MQW fabricated by MOCVD, in the (In,Ga)N/GaN layers grown by MBE $\eta$ exhibits a clear decrease with increasing $G$. For the 6 nm MQW (sample 2), the onset of this reduction is found at lower generation rates than for the MQW with thinner wells (sample 1). In sample 2, the decrease of $\eta$ is accompanied by a blueshift of the spectrum of about 40 meV, which is displayed in Fig. 4(b). For the thin (In,Ga)N/GaN MQWs (samples 1 and 3), $E_t(G)$ is almost constant within the considered $G$ range (not shown in the graph).

A completely different behavior has been observed in the GaN/(Al,Ga)N MQW (sample 4), which is summarized in Fig. 5. Here, the $G$ dependence of $\eta$ exhibits—in correspondence with Fig. 3(d)—a small but reproducible decrease with a decreasing generation rate, while $E_t(G)$ remains almost constant. Therefore, both results clearly differ from the ones for the (In,Ga)N/GaN layer systems. The normalization of $\eta$ to unity is arbitrary in this case and has no physical meaning. The increase of the quantum efficiency for higher $G$ values is obviously caused by a saturation of nonradiative recombination channels. This is a first hint that the recombination properties of the GaN/(Al,Ga)N MQWs are dominated by delocalized exciton states even at low temperatures.

In Ref. 26, we recently developed a model, in which coupled-rate equations for the density of free $n_f$ and localized excitons $n_b$ together with the density $N_b$ of localized states are self-consistently solved in conjunction with the Schrödinger and Poisson equations taking into account polarization-field screening effects. The quantum efficiencies of the free $\eta_f$ and localized excitons $\eta_b$ are defined by

$$\eta_f = \frac{\gamma_{rf} n_f}{G}, \tag{2}$$

$$\eta_b = \frac{\gamma_{rb} n_b}{G}, \tag{3}$$

where $\gamma_{rf}$ and $\gamma_{rb}$ denote the radiative recombination rates for free and bound excitons, respectively. $\gamma_{rf} = aR/T$, where $a$ denotes a constant and $R$ the overlap integral of the electron- and hole-wave functions. The total quantum efficiency $\eta$ is given by $\eta_f + \eta_b$. The fit parameters of this model are $a$, $N_b$, the localization energy $E_b$ and the nonradiative recombination rate of free excitons $\gamma_{nr}$, while the nonradiative recombination rate of bound excitons has been neglected.

The solid lines in Figs. 4(a) and 4(b) display the best fit of the experimental dependence of the quantum efficiency and transition energy on the excitation density at 5 K for the MBE-grown (In,Ga)N/GaN samples (samples 1 and 2) to the Eqs. (2) and (3). The fits are quite satisfactory, in that they reproduce the general trends very well. For the total quantum efficiency $\eta(G)$, the fits result in the following values: $aR = 90\ \mathrm{ns}^{-1}\,\mathrm{K}$ and $14\ \mathrm{ns}^{-1}\,\mathrm{K}$ for samples 1 and 2, respectively, at low excitation densities, while $N_b = 5\times10^9\ \mathrm{cm}^{-2}$, $E_b = 34$ meV, and $\gamma_{nr} = 2\ \mathrm{ns}^{-1}$ are the same for both samples.

The comparison of the experimental data with the simulations demonstrates the impact of free and bound exciton recombination as well as of electric-field screening on the quantum efficiency [cf. solid, dotted, and dashed lines for sample 2 in Fig. 4(a)]. The decrease of $\eta$ for $G > 2\times10^{18}\ \mathrm{cm}^{-2}\,\mathrm{s}^{-1}$ is due to a decrease of the quantum efficiency $\eta_b$ of the bound excitons, which is a result of the complete occupation of localized states. This is consistently linked to an increasing contribution of quasifree excitons. Those delocalized excitons can more easily find nonradiative recombination channels compared to the localized ones resulting in a decrease of the total quantum efficiency. The delocalization-related decrease of $\eta$ is accompanied by an increase of $E_t$. An increase of $\eta$ and $E_t$ due to screening of the polarization fields is predicted to occur only for high generation rates exceeding $10^{20}\ \mathrm{cm}^{-2}\,\mathrm{s}^{-1}$, which could not be reached in our experiments. The shift of the onset of the efficiency decrease toward higher values of $G$ in sample 1 compared to sample 2 is well described by our model, if $N_b$ is kept constant for both samples and the radiative recombination rate of the localized states $\gamma_{rb} = 1$ and $0.02\ \mathrm{ns}^{-1}$ for samples 1 and 2, respectively, are used, which were determined by time-resolved PL experiments.[10]

Since we can expect strong localization in the MOCVD-grown (In,Ga)N/GaN MQW (sample 3),[12,16] the experimentally attainable maximum values of $G$ are probably not sufficiently large in order to observe any delocalization-induced reduction of $\eta$. Thus, model calculations could not be performed for this sample. In the GaN/(Al,Ga)N (sample 4), the slight increase of the quantum efficiency with increasing excitation density is likely due to a saturation of nonradiative recombination channels (cf. Fig. 5) indicating weak localization.

In order to obtain further information about the influence of exciton localization on $\eta$ for our MQW structures, in particular about the difference between the weak localization in the MBE-grown GaN/(Al,Ga)N and strong localization in the MOCVD-grown (In,Ga)N/GaN QWs, we performed $T$-dependent measurements of the CL and PL intensities, which are described in the following subsection.

### B. Temperature dependence of the quantum efficiency

Figure 6 displays the integrated CL intensity of the samples 1, 3, and 4 with similar well width (cf. Table I) as a function of $T$ obtained under low-generation-rate conditions (strongly defocused electron beam). Due to a temperature-related sample drift and variations of exposure effects, the reproducibility of these temperature dependencies is rather unsatisfactory. Nevertheless, we establish a clear trend between the samples, which is well confirmed by the corresponding PL intensity dependence depicted in Fig. 7. The onset of the intensity degradation with increasing $T$ is found at the lowest $T$ for the GaN/(Al,Ga)N MQW and at the highest $T$ for the MOCVD-grown (In,Ga)N/GaN MQW. Moreover, for high temperatures, $\eta(T)$ of the MOCVD-grown sample exhibits the steepest slope indicating the largest activation energy. These data confirm that exciton localization plays a minor role in the recombination dynamics of the GaN/(Al,Ga)N MQWs (sample 4). However, in the MOCVD-grown (In,Ga)N/GaN MQW (sample 3), $\eta(T)$ indicates that exciton localization plays a significant role in the recombination dynamics of this system. Consequently, the insensitivity of $\eta$ to variations in the generation rate shown above is most probably due to exciton localization effects, which are more effective in the MOCVD-grown (In,Ga)N/GaN MQWs compared with the ones fabricated by MBE.

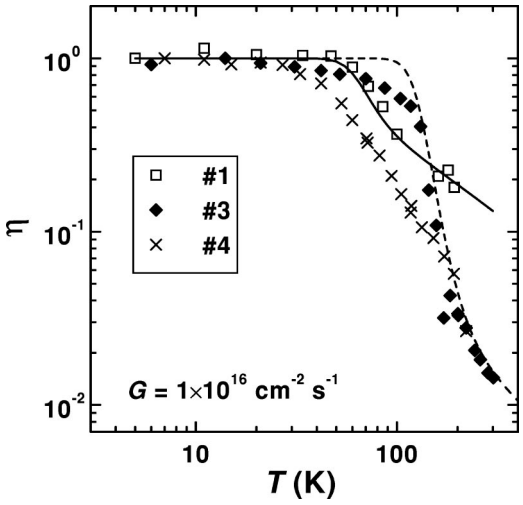


FIG. 6. Quantum efficiency of samples 1, 3, and 4 as a function of temperature. The generation rate was set to about $1\times10^{16}\ \mathrm{cm}^{-2}\,\mathrm{s}^{-1}$. The solid and dashed lines indicate the fits to a recently developed model.

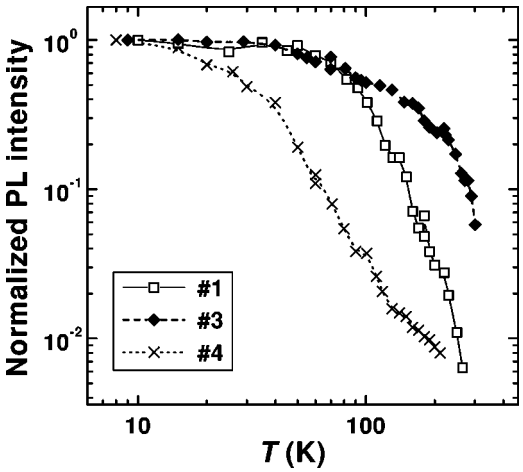


FIG. 7. Normalized PL intensity of samples 1, 3, and 4 as a function of temperature. The solid lines serve as a guide to the eye.

In order to determine the thermal activation energy of localization for samples 1 and 3, we tried to use our model to fit the experimental $T$ dependence of the CL quantum efficiency, which is shown in Fig. 6 as the dashed and solid lines. For sample 1, we used the same fit parameters mentioned above. For sample 3, the fit results in the following fit parameters: $aR=90\ \mathrm{ns}^{-1}\ \mathrm{K}$, $N_b=1\times10^{10}\ \mathrm{cm}^{-2}$, $E_b=100$ meV, and $\gamma_{nr}=22\ \mathrm{ns}^{-1}$. Clearly, $N_b$ and $E_b$ of the localized states are larger in the MOCVD-sample 3 compared with the corresponding MQW grown by MBE (sample 1).

## IV. CONCLUSIONS

In (In,Ga)N/GaN MQWs fabricated by MOCVD and MBE as well as in GaN/(Al,Ga)N MQWs grown by MBE, the generation rate dependence of the quantum efficiency indicates strong, moderate, and weak exciton localization, respectively. Fitting the experimental data to a recently developed model shows that for MBE-grown (In,Ga)N/GaN MQWs saturation of localized states leads to a decrease of the quantum efficiency and to a blueshift of the transition energy for generation rates on the order of $10^{18}$–$10^{19}\ \mathrm{cm}^{-2}\ \mathrm{s}^{-1}$. Electric-field screening is expected to affect $\eta$ and $E_t$ only for generation rates exceeding $10^{20}\ \mathrm{cm}^{-2}\,\mathrm{s}^{-1}$. Moreover, the localization energy $E_b$ has been determined to amount to 34 meV in the (In,Ga)N/GaN structures grown by MBE and to equal 100 meV in the MOCVD structure. Since the value of $E_b$ of the former is close to the calculated variation of the transition energy for a well width fluctuation of $\pm1$ monolayer, potential minima due to interface roughness can account for the observed localization phenomena in the (In,Ga)N/GaN MQWs fabricated by MBE. The much larger value of $E_b$ in the MOCVD-grown (In,Ga)N/GaN MQW suggests that alloy fluctuations have to be taken into account in order to explain the strong localization. The power and temperature dependence of $\eta$ for the GaN/(Al,Ga)N MQW is dominated by quasifree excitons even at low temperatures.

## ACKNOWLEDGMENTS

The authors would like to thank P. Waltereit and A. Thamm for fabricating the MBE samples.

[1] B. Monemar, J. P. Bergman, J. Dalfors, G. Pozina, B. E. Sernelius, P. O. Holtz, H. Amano, and I. Akasaki, MRS Internet J. Nitride Semicond. Res. **4**, 16 (1999).
[2] R. Cingolani, A. Botchkarev, H. Tang, H. Morkoç, G. Traetta, G. Coli, M. Lomascolo, A. Di Carlo, F. Della Sala, and P. Lugli, Phys. Rev. B **61**, 2711 (2000).
[3] A. Thamm, O. Brandt, J. Ringling, A. Trampert, K. H. Ploog, O. Mayrock, H.-J. Wünsche, and F. Henneberger, Phys. Rev. B **61**, 16 025 (2000).
[4] F. Della Sala, A. Di Carlo, P. Lugli, F. Bernardi, V. Fiorentini, R. Scholz, and J.-M. Jancu, Appl. Phys. Lett. **74**, 2002 (1999).
[5] K. P. O'Donnell, R. W. Martin, and P. G. Middleton, Phys. Rev. Lett. **82**, 237 (1999).
[6] Y.-S. Lin, K.-J. Ma, C. Hsu, S.-W. Feng, Y.-C. Cheng, C.-C. Liao, C. C. Yang, C.-C. Chou, C.-M. Lee, and J.-I. Chyi, Appl. Phys. Lett. **77**, 2988 (2000).
[7] Y. Narukawa, Y. Kawakami, M. Funato, Shizuo Fujita, Shigeo Fujita, and S. Nakamura, Appl. Phys. Lett. **70**, 981 (1997).
[8] A. Vertikov, A. V. Nurmikko, K. Doverspike, G. Bulman, and J. Edmond, Appl. Phys. Lett. **73**, 493 (1998).
[9] U. Jahn, O. Brandt, A. Trampert, P. Waltereit, R. Hey, and K. H. Ploog, Mater. Sci. Eng. B **91–92**, 329 (2002).
[10] P. Waltereit, O. Brandt, J. Ringling, and K. H. Ploog, Phys. Rev. B **64**, 245305 (2001).
[11] S. F. Chichibu, T. Sota, K. Wada, S. P. DenBaars, and S. Nakamura, MRS Internet J. Nitride Semicond. Res. **4S1**, G2.7 (1999).
[12] Y. Narukawa, Y. Kawakami, Shizuo Fujita, Shigeo Fujita, and S. Nakamura, Phys. Rev. B **55**, R1938 (1997).
[13] X. Zhang, D. H. Rich, J. T. Kobayashi, N. P. Kobayashi, and P. D. Dapkus, Appl. Phys. Lett. **73**, 1430 (1998).
[14] M. Pophristic, F. H. Long, C. Tran, and I. T. Ferguson, MRS Internet J. Nitride Semicond. Res. **5S1**, W11.58 (2000).
[15] Y. Narukawa, S. Saijou, Y. Kawakami, S. Fujita, T. Mukai, and S. Nakamura, Appl. Phys. Lett. **74**, 558 (1999).
[16] Y. Narukawa, Y. Kawakami, S. Fujita, and S. Nakamura, Phys. Rev. B **59**, 10 283 (1999).
[17] E. Berkowicz, D. Gershoni, G. Bahir, E. Lakin, D. Shilo, E. Zolotoyabko, A. C. Abare, S. P. DenBaars, and L. A. Coldren, Phys. Rev. B **61**, 10 994 (2000).
[18] P. Lefebvre, J. Allègre, B. Gil, A. Kavokine, H. Mathieu, W. Kim, A. Salvador, A. Botchkarev, and H. Morkoç, Phys. Rev. B **57**, R9447 (1998).
[19] A. Hangleiter, J. S. Im, H. Kollmer, S. Heppel, J. Off, and F. Scholz, MRS Internet J. Nitride Semicond. Res. **3**, 15 (1998).
[20] J. C. Harris, T. Someya, S. Kako, K. Hoshino, and Y. Arakawa, Appl. Phys. Lett. **77**, 1005 (2000).
[21] P. Riblet, H. Hirayama, A. Kinoshita, A. Hirata, T. Sugano, and Y. Aoyagi, Appl. Phys. Lett. **75**, 2241 (1999).
[22] M. Leroux, N. Grandjean, M. Laügt, J. Massies, B. Gil, P. Lefebvre, and P. Bigenwald, Phys. Rev. B **58**, R13 371 (1998).
[23] R. Lager, J. Simon, V. Ortiz, N. T. Pelekanos, A. Barski, R. André, and M. Godlewski Appl. Phys. Lett. **74**, 3827 (1999).
[24] S.-H. Park and S.-L. Chuang, Appl. Phys. Lett. **76**, 1981 (2000).
[25] A. Bonfiglio, M. Lomascolo, G. Traetta, R. Cingolani, A. Di Carlo, F. Della Sala, P. Lugli, A. Botchkarev, and H. Morkoç, J. Appl. Phys. **87**, 2289 (2000).
[26] S. Dhar, U. Jahn, O. Brandt, P. Waltereit, and K. H. Ploog, Appl. Phys. Lett. **81**, 673 (2002).
[27] G. Beadie, W. S. Rabinovich, A. E. Wickenden, D. D. Koleske, S. C. Binari, and J. A. Freitas, Jr., Appl. Phys. Lett. **71**, 1092 (1997).
[28] M. T. Hirsch, J. A. Wolk, W. Walukiewicz, and E. E. Haller, Appl. Phys. Lett. **71**, 1098 (1997).
[29] C. H. Qiu and J. I. Pankove, Appl. Phys. Lett. **70**, 1983 (1997).
[30] C. V. Reddy, K. Balakrishnan, O. Okumura, and S. Yoshida, Appl. Phys. Lett. **73**, 244 (1998).
[31] A. Y. Polyakov, N. B. Smirnov, A. V. Govorkov, M. Shin, M. Skowronski, and D. W. Greve, J. Appl. Phys. **84**, 870 (1998).
[32] X. Z. Dang, C. D. Wang, E. T. Yu, K. S. Boutros, and J. M. Redwing, Appl. Phys. Lett. **72**, 2745 (1998).
[33] H. C. Yang, T. Y. Lin, and Y. F. Chen, Appl. Phys. Lett. **78**, 338 (2001).
[34] S. J. Chung, O. H. Cha, Y. S. Kim, C.-H. Hong, H. J. Lee, M. S. Jeong, J. O. White,and E.-K. Suh, J. Appl. Phys. **89**, 5454 (2001).
[35] I. K. Shmagin, J. F. Muth, R. M. Kolbas, M. P. Mack, A. C. Abare, S. Keller, L. A. Coldren, U. K. Mishra, and S. P. DenBaars, Appl. Phys. Lett. **71**, 1455 (1997).
[36] Y. C. Chang, A. L. Cai, M. A. L. Johnson, J. F. Muth, R. M. Kolbas, Z. J. Reitmeier, S. Einfeldt, and R. F. Davis, Appl. Phys. Lett. **80**, 2675 (2002).
[37] S. Dhar and S. Ghosh, Appl. Phys. Lett. **80**, 4519 (2002).
[38] Y. C. Chang, A. E. Oberhofer, J. F. Muth, R. M. Kolbas, and R. F. Davis, Appl. Phys. Lett. **79**, 281 (2001).
[39] R. Pecharromán-Gallego, P. R. Edwards, R. W. Martin, and I. M. Watson, Mater. Sci. Eng. B **93**, 94 (2002).
[40] C. J. Wu and D. B. Wittry, J. Appl. Phys. **49**, 2827 (1978).